Available online at www.sciencedirect.com
ScienceDirect
Bioorganic Chemistry 35 (2007) 50–58
BIOORGANIC CHEMISTRY
www.elsevier.com/locate/bioorg

Mechanistic differences between *in vitro* assays for hydrazone-based small molecule inhibitors of anthrax lethal factor

M. Leslie Hanna, Theodore M. Tarasow, Julie Perkins *

Chemistry and Materials Science Directorate, Lawrence Livermore National Laboratory, 7000 East Avenue, Livermore, CA 94551, USA

Received 27 June 2006
Available online 1 September 2006

Abstract

A systematically generated series of hydrazones were analyzed as potential inhibitors of anthrax lethal factor. The hydrazones were screened using one UV-based and two fluorescence-based *in vitro* assays. The study identified several inhibitors with IC_{50} values in the micromolar range, and importantly, significant differences in the types of inhibition were observed with the different assays.

Keywords: Anthrax; Lethal factor; Inhibitor; Hydrazone

1. Introduction

Inhalation of *Bacillus anthracis* spores is often fatal if not appropriately treated in a timely fashion. Inhaled spores in the lung alveoli are phagocytosed by alveolar macrophages and transported to the lymph nodes, where the spores germinate and multiply. The bacteria release a toxin that kills host macrophages, disabling the host immune system and thereby allowing the bacteria to escape the lymphonode defense barrier to reach the blood system causing bacteraemia and toxaemia, which rapidly kills the host [1,2].

* Corresponding author. Fax: +1 925 422 3570.
E-mail address: perkins14@llnl.gov (J. Perkins).

0045-2068/$ - see front matter
doi:10.1016/j.bioorg.2006.07.004

Antibiotic treatment can be effective following low dose exposure. However, there is no effective method to treat an established infection, as the toxin continues to damage the host even after the bacteria may have been killed by antibiotic treatment. The release of *B. anthracis* spores as an act of terrorism necessitates the search for effective treatments to inhibit the action of the toxin, which could be used alone or in combination with antibiotics to treat high dose exposure or established infections.

Anthrax toxin consists of three proteins: protective antigen (PA) [3,4], edema factor (EF) [5] and lethal factor (LF). PA is responsible for binding to cell surface receptors where it is proteolitically cleaved to produce a 20 kDa fragment and a 63 kDa fragment [6,7]. Following cleavage, the 63 kDa fragment heptamarises to form a prepore that, after binding either LF or EF, is transported into the cell by receptor-mediated endocytosis [8]. EF is a calmodulin-dependant adenylyl cyclase that can elevate intracellular cAMP to pathological levels [5,9]. LF is a zinc-dependant metalloprotease that cleaves mitogen-activated protein kinase kinases (MAPKK) at their amino termini [10–12]. Cleavage disrupts the ability of these kinases to interact with and phosphorylate downstream substrates, which leads finally to macrophage lysis *via* a mechanism not entirely understood to date.[13] As outlined previously, the inhibition of LF proteolytic activity is a promising method for treating exposure to *B. anthracis* spores [14] and inhibitors may also act as the molecular recognition unit in an anthrax toxin detection assay.

Assays based on UV, fluorescence and mass spectrometry detection of cleavage products are commonly used for the analysis of proteolytic activity and the discovery of protease inhibitors. Several groups have reported the use of *in vitro* protease assays to identify LF inhibitors and in some cases, effective inhibitors were further analyzed in cell-based assays [15–24]. In an elegant study to demonstrate the use of self-assembled monolayer mass spectrometry screening for protease inhibitors, Mrksich and coworkers [25] identified a hydrazone-based small molecule as an effective non-competitive inhibitor of LF.

In this study, the hydrazone bond was used as a foundation to generate a series of libraries to investigate the structure-activity relationships of hydrazone-based inhibitors and LF using a UV-based *in vitro* assay. The most effective hydrazone-based LF inhibitors were further evaluated using two fluorescence-based *in vitro* assays and the mechanism of the inhibitors were compared over all experiments. Inhibition mechanism differences were observed between the assay that most accurately reflects the native peptide bond hydrolysis and the two assays that utilize unnatural peptide bond cleavage to release optical reporter groups. The differences demonstrate that caution should be taken when interpreting inhibition data based upon unnatural protease substrates and helps to identify the site of inhibition of the hydrazone-based LF inhibitors.

2. Materials and methods

2.1. Hydrazone formation

Component aldehydes and hydrazides were purchased from Sigma, Aldrich, Avacodo, Alfa or TCI and used as received. Concentrated solutions of the aldehydes and hydrazides were prepared in DMSO, and in most cases, were diluted to 20 mM. Some molecules were restricted in amount available or solubility and these were prepared at lower concentrations. The aldehyde and hydrazide solutions were mixed in 1:1 ratios (except with bis-hydrazide **h**, where a 2:1 ratio of aldehyde: hydrazide was used) and agitated in the dark

overnight in the presence of 0.1% formic acid. The resultant hydrazones were subsequently screened against LF following dilution in DMSO to the appropriate concentration. The hydrazone formation was confirmed with numerous aldehyde/hydrazide combinations in d_6-DMSO using Nuclear Magnetic Resonance spectroscopy.

2.2. Control experiments

A representative number of aldehydes and hydrazides were screened in a similar manner to the hydrazones to confirm that hydrazone formation was required for inhibition. No inhibition was observed with the representative component aldehydes and hydrazides.

2.3. p-Nitroaniline (p-NA) release UV assay [25]

The substrate, Ac-NleKKKKVLP-*p*NA, was synthesized as described previously [25]. 0.05–0.2 μg of LF was pre-incubated for 5 min with 0–10 μM inhibitor in 25 mM HEPES, pH 7.0 containing 10 mM NaCl, 5 mM $MgCl_2$, 50 μM $ZnCl_2$, 50 μM $CaCl_2$ and 0.5% DMSO at room temperature. Aliquots (97.5 μL) were added to duplicate wells of a 96 well plate containing 2.5 μL of 10 mM substrate, Ac-NleKKKKVLP-*p*NA (final concentration 0.25 mM), in the same buffer. The release of *p*-NA was monitored at 385 nm at 1–2 min intervals for 20 min (using a Bio-Tek Synergy HT plate reader) and quantified using a *p*-NA standard.

2.4. Coumarin release fluorescent assay

AcGYβARRRRRRRRVLR-7-AMC was commercially synthesized as described previously [22]. Assays were carried out as described previously, [22], except using HEPES buffer (same as in MAPKKide experiments) in place of sodium phosphate for continuity in the experimental procedures. 100 μM inhibitor was used in each experiment to achieve >50% inhibition. The probe has an excitation wavelength of 360 nm and emission wavelength of 460 nm. Significant interference from the hydrazone inhibitors in the fluorescence of the released coumarin was observed. This background was subtracted by running a non-enzymatic control experiment for each hydrazone analyzed.

2.5. MAPKKide assay

These assays were carried out as described by Pellecchia and coworkers [23] using 100 μM inhibitor to achieve >50% inhibition. MAPKKide peptide substrate (DABCYL/FITC) has an excitation wavelength of 485 nm and an emission wavelength of 590 nm, was obtained from List Biological Laboratories and used as received.

3. Results and discussion

The structure of the hydrazone LF inhibitor identified by Mrksich and coworkers [25] is shown in Fig. 1. To carry out a structure–activity study to identify more potent hydrazone inhibitors and map the non-covalent interactions between enzyme and inhibitor, hydrazones formed from all possible combinations of a broad range of component aldehydes and hydrazides were screened using a *p*-NA release, UV-based assay. The structures of the

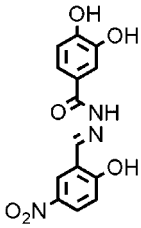

Fig. 1. Structure of LF hydrazone-based inhibitor identified by Mrksich and coworkers (**1a** in Table 1).

aldehydes and hydrazides used in this initial screen are shown in Fig. 2 and include the components of the hydrazone in Fig. 1—2-hydroxy-5-nitro-benzaldehyde and 3,4-dihydroxy-benzhydrazide.

Only hydrazones with a 2-hydroxy-5-nitro-benzaldehyde component showed any significant inhibitory effect. Therefore, a further series of hydrazones formed using aldehydes differentially substituted only in the 2 and/or 5 positions were analyzed. These aldehydes are listed in the supplementary material. All inhibitors identified in the second screen consistently had a 2-position substitution of the aldehyde component, and the substituent was often an OH group, which may participate in coordination to the zinc ion, creating an inhibitory effect. This second screen yielded more inhibitors and therefore, this larger library of 2-substituted, and in some cases also 5-substituted, aldehydes were used as the basis to screen a broader range of component hydrazides (shown in supplementary material).

The components of all the hydrazones that showed an inhibitory effect in the *p*-NA UV assay (including the lead candidate hydrazone in Fig. 1) are shown in Table 1. Subsequently, these lead hydrazone inhibitors were further analyzed using a fluorescence-based assay

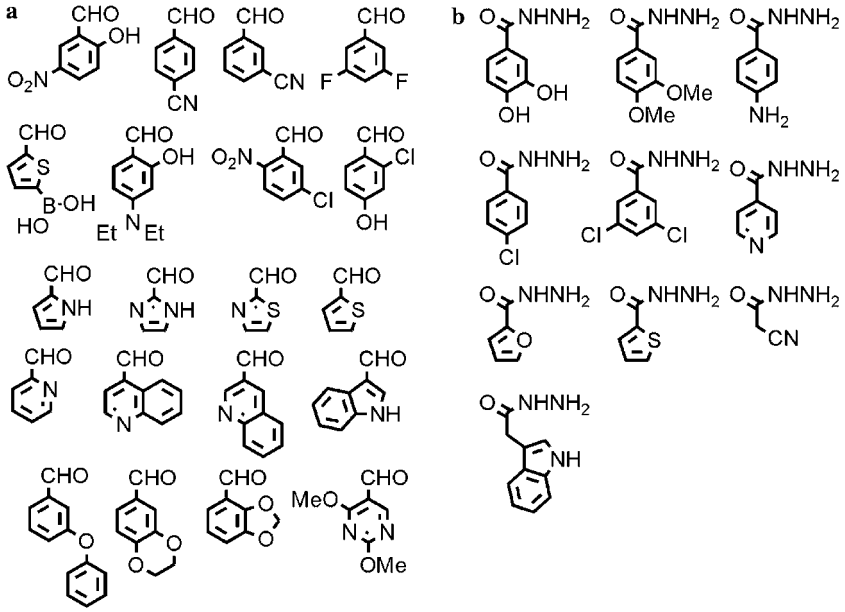

Fig. 2. Component (a) aldehydes and (b) hydrazides of hydrazone inhibitors examined during an initial broad screen using the *p*-NA UV-based assay.

Table 1
LF inhibition

		a 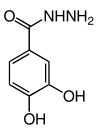	**b** 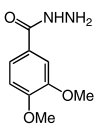	**c** 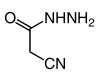	**d** 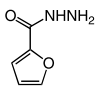	**e** 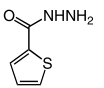	**f** 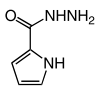	**g** 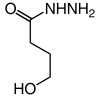	**h** 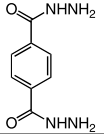	**i** 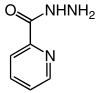	**j** 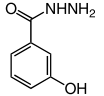
1	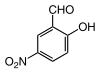	+++ OO XX	+++ OOO X	++ OOO XX	+++ OO X	+++ OOO XX	+ X		++	+++ O	+++ O
2	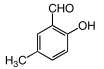	 XX	+	+ OO	++ X	+ O	+ X	+	++ OOO XXX	+++	
3		O		O			++	+	++ OOO XXX	++	
4		 OO XXX					 XXX	+			X
5		 O X			++				+ O X		
6		 O		O	+				+		
7		+ O X		O					++ OOO XXX	++	
8	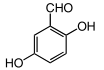	+ OO XX	+	OO	OOO		+ X	O	+++ OO XXX		OO

1–8; aldehydes and **a–j**; hydrazides used to construct hydrazone LF inhibitors. +, *p*-NA assay (10 μM inhibitor); o, AcGY*β*ARRRRRRRRVLR-7-AMC assay (100 μM inhibitor); x, MAPKKide assay (100 μM inhibitor). Three symbols <50% activity remaining; two symbols 50–75% activity remaining; one symbol 75–80% activity remaining. No symbols, no significant inhibitory effect observed. The inhibitory effects of the highlighted inhibitors **1a**, **2h**, **3h** and **7h** were assessed more thoroughly.

previously described by Montecucco and coworkers [22]. In this case, many of the most potent inhibitors contained component aldehyde **1** or aldehyde **8**, and hydrazide **a** or hydrazide **h**.

Finally, the hydrazones in Table 1 were further analyzed using the commercially available MAPKKide FRET-based assay. Similarly to the coumarin assay, the MAPKKide assay identified strongest inhibitor candidates composed of aldehyde **1**, hydrazide **a** (although a little weaker) and hydrazide **h**. The inclusion of hydrazide **h** gave inhibitors of a long, narrow, hydrophobic nature, and this is consistent with the observations of Panchal et al., [21] where they observed their hydrophobic inhibitors lie over the catalytic zinc binding site, blocking the activity of the protease. The MAPKKide assay uses a peptide

Table 2
Four MAPKK residues flanking the LF cleavage site [12,26]

	Cleavage							
	P4	P3	P2	P1	P1′	P2′	P3′	P4′
MKK-1	K	P	T	P	I	Q	L	N
MKK-2	P	V	L	P	A	L	T	I
MKK-3	K	D	L	R	I	S	C	M
MKK-4	K	A	L	K	L	N	F	A
MKK-4	S	T	A	R	F	T	L	N
MKK-6	P	G	L	K	I	P	K	E
MKK-7	P	T	L	Q	L	P	L	A
MKK-7	H	M	L	G	L	P	S	T

Cleavage occurs between P and P′ residues.

Table 3
IC_{50} values and structures of hydrazone inhibitors highlighted in Table 1

Assay	IC_{50} (μM) Hydrazone inhibitor			
	1a	**2h**	**3h**	**7h**
p-NA	8 ± 0.2	85 ± 3	45 ± 1	40 ± 1
Coumarin	150 ± 5	90 ± 3	50 ± 2	70 ± 2
MAPPKide	200 ± 18	80 ± 7	50 ± 5	50 ± 5

Data is an average of two repeats.

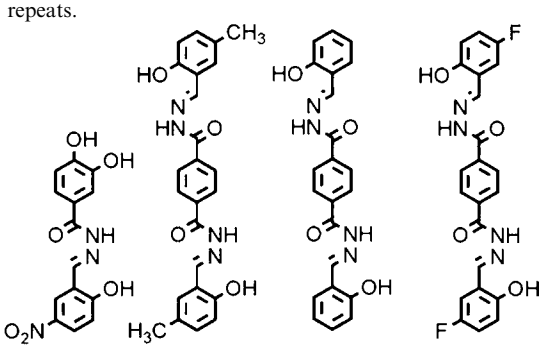

substrate containing a natural cleavage site for LF with natural amino acid residues flanking the scissile bond, and consequently interacts with the entire LF active site [26]. Table 2 illustrates representative examples of amino acids located on either side of the LF cleavage site of natural MAPKK substrates, where cleavage is between the P1 and P1′ sites [12,26].

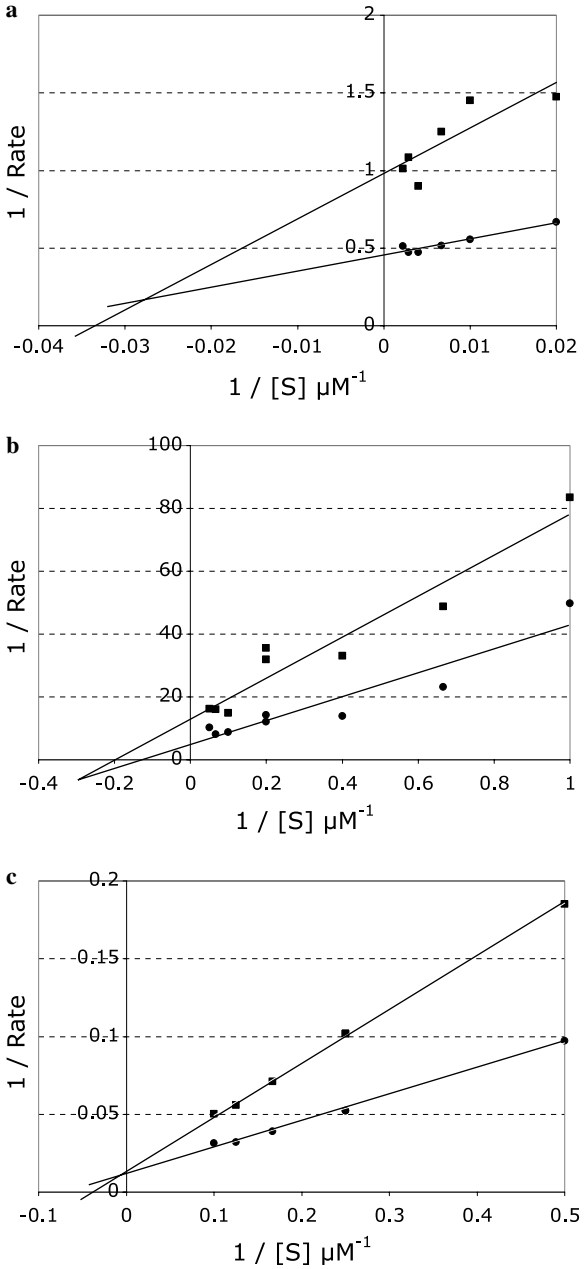

Fig. 3. Lineweaver–Burke plots of inhibitor **2h** for each assay. (a) *p*-NA assay — **2h** at 10 μM (b) Coumarin assay — **2h** at 100 μM (c) MAPKKide assay — **2h** at 100 μM. Data is an average of two repeats.

In contrast, the *p*-NA- and coumarin-based assays employ substrates that only contain amino acid residues in the P sites. It is unclear how the unnatural optical tag interacts with the active site, although given the nature of the substrate and the active site, the tag is likely to at least partially inhabit the P1′ site. Cleavage at the terminus of the peptide substrate (P1 site) releases the unnatural UV-active or fluorescent molecule. Based on these substrate differences, any active site inhibitor in the FRET assay would result in competitive inhibition, whereas in the *p*-NA and coumarin assays, active site inhibitors could display competitive (binding in the P sites) or non-competitive (binding in the P′ sites) inhibition depending on what portion of the LF active site they interact with.

Table 3 shows the IC_{50} and the hydrazone structures of the selection of the inhibitors highlighted in Table 1. In this case, 0.5 μg of LF enzyme was used to obtain these values. The inhibitors identified in this study do not show a significantly enhanced inhibitory effect over the original lead candidate **1a** (8 μM in this study). When the *p*-NA assay was repeated at lower enzyme concentration (0.17 μg), an IC_{50} of 2 μM for **1a** was obtained, consistent with previously reported results.[25] A representative example (inhibitor **2h**) of Lineweaver–Burke plots for the *p*-NA and coumarin assays (Fig. 3a and b respectively) shows the inhibition mechanism is not distinct. The lines clearly intersect to the left of the *y*-axis but not on the x-axis, suggesting a mixed mode of inhibition. However, the inhibitors exhibit competitive inhibition with the MAPKKide assay as shown by a representative example (inhibitor **2h**) of a Lineweaver–Burke plot in Fig. 3c. These differences suggest the hydrazone inhibitors are binding in the P′ sites since occupation of these sites would directly compete for active site binding with the MAPKKide substrate, but not necessarily the *p*-NA and coumarin substrates. The *p*-NA and coumarin leaving groups may interact with the P′ sites to some extent, causing the mixed mode of inhibition to be observed. For future work, these results indicate that more potent inhibitors may be discovered by extending the hydrazone inhibitors to bind to the P sites.

These experiments highlight the quite different results that can be obtained when using different *in vitro* assays to identify protease inhibitors. Importantly, biochemical investigations using different substrates can yield information on inhibition mechanisms and identify sites of inhibitor–enzyme interaction.

4. Conclusions

In summary, three *in vitro* assays were used to analyze a series of hydrazones for their inhibitory effects on the proteolytic action of anthrax LF. A number of inhibitors were identified, although not with significantly enhanced inhibitory effect over the initial lead compound. However, notable differences in the types of inhibition observed using the different assays identified the likely binding site of the inhibitors, and these observations will be taken into account in future protease inhibitor assay development.

Acknowledgments

This work was carried out under the auspices of the US Department of Energy by the University of California, Lawrence Livermore National Laboratory under Contract W-7405-Eng-48 with financial support from the Laboratory Directed Research and Development fund. The authors thank Sandra L. McCutchen-Maloney and Todd H. Corzett (LLNL) for access and assistance with the UV/fluorescence plate reader. The authors

thank Erica L. Gjersing and Julie L. Herberg (LLNL) for assistance in acquiring NMR spectra.

Appendix A. Supplementary data

Supplementary data associated with this article can be found, in the online version, at doi:10.1016/j.bioorg.2006.07.004.

References

[1] M. Mock, A. Fouet, Annu. Rev. Microbiol. 55 (2001) 647–671.
[2] T.C. Dixon, M. Meselson, J. Guillemin, P.C. Hanna, N. Engl, J. Med. 341 (1999) 815–826.
[3] K.A. Bradley, J. Mogridge, M. Mourez, R.J. Collier, J.A.T. Young, Nature 414 (2001) 225–229.
[4] K.A. Bradley, J.A.T. Young, Biochem. Pharmacol. 65 (2003) 309–314.
[5] S.H. Leppla, Proc. Natl. Acad. Sci. Biol. 79 (1982) 3162–3166.
[6] S.S. Molloy, P.A. Bresnahan, S.H. Leppla, K.R. Klimpel, G. Thomas, J. Biol. Chem. 267 (1992) 16396–16402.
[7] K.R. Klimpel, S.S. Molloy, G. Thomas, S.H. Leppla, Proc. Natl. Acad. Sci. USA 89 (1992) 10277–10281.
[8] J. Mogridge, K. Cunningham, R.J. Collier, Biochemistry 41 (2002) 1079–1082.
[9] C.L. Drum, S.Z. Yan, J. Bard, Y.Q. Shen, D. Lu, S. Soelalman, Z. Grabarek, A. Bohm, W.J. Tang, Nature 415 (2002) 396–402.
[10] N.S. Duesbery, C.P. Webb, S.H. Leppla, V.M. Gordon, K.R. Klimpel, T.D. Copeland, N.G. Ahn, M.K. Oskarsson, K. Fukasawa, K.D. Paull, G.F. Vande Woude, Science 280 (1998) 734–737.
[11] G. Vitale, R. Pellizzari, C. Recchi, G. Napolitani, M. Mock, C. Montecucco, Biochem. Biophys. Res. Commun. 248 (1998) 706–711.
[12] G. Vitale, L. Bernardi, G. Napolitani, M. Mock, C. Montecucco, Biochem. J. 352 (2000) 739–745.
[13] J.M. Park, F.R. Greten, Z.W. Li, M. Karin, Science 297 (2002) 2048–2051.
[14] B.R. Sellman, M. Mourez, R.J. Collier, Science 292 (2001) 695–697.
[15] S.K. Grant, J.G. Sklar, R.T. Cummings, J. Biomol. Screen. 7 (2002) 531–540.
[16] M. Fridman, V. Belakhov, L.V. Lee, F.S. Liang, C.H. Wong, T. Baasov, Angew. Chem. Int. Ed. Engl. 44 (2005) 447–452.
[17] C. Montecucco, F. Tonello, G. Zanotti, Trends Biochem. Sci. 29 (2004) 282–285.
[18] W.L. Shoop, Y. Xiong, J. Wiltsie, A. Woods, J. Guo, J.V. Pivnichny, T. Felcetto, B.F. Michael, A. Bansal, R.T. Cummings, B.R. Cunningham, A.M. Friedlander, C.M. Douglas, S.B. Patel, D. Wisniewski, G. Scapin, S.P. Salowe, D.M. Zaller, K.T. Chapman, E.M. Scolnick, D.M. Schmatz, K. Bartizal, M. MacCoss, J.D. Hermes, Proc. Natl. Acad. Sci. USA 102 (2005) 7958–7963.
[19] Y.S. Xiong, J. Wiltsie, A. Woods, J. Guo, J.V. Pivnichny, W. Tang, A. Bansal, R.T. Cummings, B.R. Cunningham, A.M. Friedlander, C.M. Douglas, S.P. Salowe, D.M. Zaller, E.M. Scolnick, D.M. Schmatz, K. Bartizal, J.D. Hermes, M. MacCoss, K.T. Chapman, Bioorg. Med. Chem. Lett. 16 (2006) 964–968.
[20] R.T. Cummings, S.P. Salowe, B.R. Cunningham, J. Wiltsie, Y.W. Park, L.M. Sonatore, D. Wisniewski, C.M. Douglas, J.D. Hermes, E.M. Scolnick, Proc. Natl. Acad. Sci. USA 99 (2002) 6603–6606.
[21] R.G. Panchal, A.R. Hermone, T.L. Nguyen, T.Y. Wong, R. Schwarzenbacher, J. Schmidt, D. Lane, C. McGrath, B.E. Turk, J. Burnett, M.J. Aman, S. Little, E.A. Sausville, D.W. Zaharevitz, L.C. Cantley, R.C. Liddington, R. Gussio, S. Bavari, Nat. Struct. Mol. Biol. 11 (2004) 67–72.
[22] F. Tonello, M. Seveso, O. Marin, M. Mock, C. Montecucco, Nature 418 (2002) 386.
[23] M. Forino, S. Johnson, T.Y. Wong, D.V. Rozanov, A.Y. Savinov, W. Li, R. Fattorusso, B. Becattini, A.J. Orry, D.W. Jung, R.A. Abagyan, J.W. Smith, K. Alibek, R.C. Liddington, A.Y. Strongin, M. Pellecchia, Proc. Natl. Acad. Sci. USA 102 (2005) 9499–9504.
[24] S.L. Johnson, D. Jung, M. Forino, Y. Chen, A. Satterthwait, D.V. Rozanov, A.Y. Strongin, M. Pellecchia, J. Med. Chem. 49 (2006) 27–30.
[25] D.H. Min, W.J. Tang, M. Mrksich, Nat. Biotechnol. 22 (2004) 717–723.
[26] B.E. Turk, T.Y. Wong, R. Schwarzenbacher, E.T. Jarrell, S.H. Leppla, R.J. Collier, R.C. Liddington, L.C. Cantley, Nat. Struct. Mol. Biol. 11 (2004) 60–66.